The Astrophysical Journal, 633:205–209, 2005 November 1

THE CLOSEST VIEW OF A DWARF GALAXY: NEW EVIDENCE ON THE NATURE OF THE CANIS MAJOR OVERDENSITY

David Martínez-Delgado,[1,2] David J. Butler,[1] Hans-Walter Rix,[1] Y. Isabel Franco,[1]
Jorge Peñarrubia,[1] Emilio J. Alfaro,[2] and Dana I. Dinescu[3]
Received 2004 October 25; accepted 2005 June 3

ABSTRACT

We present the first deep color-magnitude diagram of the putative central region ($0.^\circ5 \times 0.^\circ5$) of the Canis Major stellar overdensity ($l,\ b$) = (240, −8) found recently by Martin and coworkers, which has been proposed as the remnant of a dwarf satellite accreted onto the Milky Way on a near-equatorial orbit. We find a narrow (in apparent magnitude) main sequence extending 6 mag below the turnoff to our limiting magnitude of $B \sim 24.5$ mag. This main sequence has very high contrast (>3) with respect to the thin/thick disk/halo background; its narrowness at brighter magnitudes clearly implies the presence of a distinct and possibly still bound stellar system. We derived the line-of-sight size ($r_{1/2}$) of this system based on the B-band width of the lower main sequence, obtaining 0.94 ± 0.18 (random) ± 0.18 (systematic) kpc. That size matches a model prediction for the main body of the parent galaxy of the Monoceros tidal stream. The high-density contrast and limited spatial extent in the radial direction are very hard to reconcile with the alternative explanation put forward to explain the Canis Major stellar overdensity: a flared or warped Galactic disk viewed in projection, as found in the recent work of Momany and coworkers. We also derived a central surface brightness of $\mu_{V,0} = 23.3 \pm 0.1$ mag arcsec^{-2} and an absolute magnitude of $M_V = -14.5 \pm 0.1$ mag. These values place the Canis Major object in the category of dwarf galaxy, considering the L_V-size and $M_V - \mu_V$ planes for such objects. However, like the Sagittarius dwarf, it is an outlier in the [Fe/H] $- M_V$ plane in the sense that it is too metal-rich for its estimated absolute magnitude. This suggests that the main mechanism driving its recent and current star formation history (possibly tidal stripping) is different from that of isolated dwarfs.

Subject headings: galaxies: dwarf — galaxies: individual (Canis Major) — galaxies: stellar content — galaxies: structure — Galaxy: structure

Online material: color figure

1. INTRODUCTION

The Milky Way offers a unique laboratory for testing the hierarchical galaxy formation scenario through direct evidence of past merging and tidal disruption events, which result in extensive stellar streams or large-scale substructures in the Galactic halo or even in the disk (see Navarro 2004 and references therein). Resolving such tidal streams into stars and measuring the phase-space coordinates for these stars provides a fossil dynamical accretion record of unparalleled accuracy. These can be directly compared with N-body simulations in order to reconstruct their dynamical history and their impact on the Milky Way at present and recent epochs.

Recently, the Sloan Digital Sky Survey (SDSS) team reported the discovery of a coherent giant stellar structure at low galactic latitudes (Newberg et al. 2003; Yanny et al. 2003), which appears to form a ring around the Milky Way. Since then, there has been a tremendous amount of follow-up observational effort probing its structure and kinematics in order to understand its origin (see Majewski 2004 and references therein). N-body simulations (Martin et al. 2004a; Peñarrubia et al. 2005) show that this ring structure can be naturally attributed to the tidal stream of a dwarf galaxy (named the Monoceros tidal stream, or the Galactic Anticenter tidal stream). If this stellar overdensity ring is a tidal tail feature, it must have had a "parent" galaxy, which may or may not be completely disrupted by now. The existence and location of such a parent galaxy is still controversial; the best candidate is the Canis Major (CMa) dwarf galaxy, a strong, ellipsoidal overdensity of red giant stars discovered in its namesake constellation by Martin et al. (2004a) from an analysis of the Two Micron All Sky Survey (2MASS). Bellazzini et al. (2004) presented a color-magnitude diagram (CMD) of the surroundings of the candidate CMa dwarf, concluding that the system is situated at 8 ± 1 kpc from the Sun and that it is composed of a metal-rich, intermediate-age stellar population. As CMa is only $\sim 8^\circ$ from the Galactic plane, Momany et al. (2004) suggested an alternative interpretation, namely, that this overdensity is the signature of the Galactic warp in this direction of the sky and not a distinct satellite. However, Martin et al. (2004b) reported a narrow distribution of radial velocities for the center of this structure and argued on this basis for the interpretation of CMa as an accreted dwarf satellite remnant in an orbit near the Galactic plane.

To help discriminate between these two hypotheses, accreted dwarf galaxy or stellar warp, we present here deep broadband photometry of the CMa center. As our results confirm and greatly strengthen the case that the stellar overdensity toward CMa is part of a distinct dwarf galaxy, we refer to it as "CMa dwarf" throughout.

2. OBSERVATIONS AND DATA REDUCTION

Our observations were carried out in B and R Johnson-Cousins filters with the 2.2 m European Southern Observatory (ESO) Max-Planck-Gesellschaft (MPG) telescope at the La Silla Observatory (Chile) in service mode during 2003 December 14–17. We used the Wide Field Imager (WFI) installed at the prime focus, which holds eight 2046×4098 pixel EEV chips, with

[1] Max-Planck Institut fur Astronomie, Königstuhl, 17 D-69117 Heidelberg, Germany.
[2] Instituto de Astrofísica de Andalucía (CSIC), Granada, Spain.
[3] Astronomy Department, Yale University, New Haven, CT.

a scale of 0.″238 pixel^{-1}. Our field covers a total area of about 0.25 deg^2 and is centered at Galactic coordinates $(l, b) = (240.^\circ15, -8.^\circ07)$, which is, within the uncertainties, the nominal center of the CMa overdensity given by Martin et al. (2004a). The total exposure times were 3700 and 2700 s in B and R, respectively. A shorter exposure of 100 s in both bands was also taken to recover the brighter part of the CMD.

Bias and flat-field corrections were done with IRAF. DAOPHOT and ALLSTAR (Stetson 1994) were used to obtain the photometry of the resolved stars. Aperture corrections were estimated using a set of about 50 isolated, bright stars in the CMa frame, with a variance of $\sigma \sim 0.001$. Transformation of the instrumental magnitudes into the standard photometric system were obtained from observations of the Landolt standard field SA95 taken during two photometric nights bracketing our observations, using the atmospheric extinction coefficients estimated on 2003 November 8.[4] Putting all the errors together, the total zero-point uncertainty of our photometry can be estimated to be about $\sigma = 0.05$ for $B - R$ and $\sigma = 0.07$ for individual bands. The resulting catalog of stars was filtered using the error parameters given by ALLSTAR, retaining only stars with acceptable CHI and SHARP parameters, and $\sigma_B < 0.2$ and $\sigma_R < 0.2$.

Artificial star tests were performed in the usual way (see Aparicio et al. 2001), using a total of 20,000 artificial stars to check the observational effects and estimate the completeness factor as a function of magnitude.

3. THE COLOR-MAGNITUDE DIAGRAM

Figure 1*a* shows the $[B - R, R]$ CMD of the center of the possible CMa dwarf based on our $t_{\rm exp} = 100$ s data. The stellar densities in this CMD confirm immediately that the distribution of stars in the Milky Way in this low-latitude direction grossly deviates from the expectations of a smooth thin/thick halo distribution: there is a conspicuous main-sequence (MS) feature (labeled "MS" in Fig. 1*b*) with a possible arc-shaped turnoff at $R = 18.48 \pm 0.11$ mag. The $B - R$ color used on our CMD provides the separation of the redder plume populated by thick disk stars {the parallel sequence running from $[R,\ (B - R)] \sim (15, 1.0)$ to $[R,\ (B - R)] \sim (19, 1.6)$} from this MS feature, which is about $\sim$0.2 mag bluer at $R \sim 18$. In addition, a second plume of possible MS stars (labeled "BP" in Fig. 1*b*) is observed extending brighter and bluer than the MS turnoff and reaching $R \simeq 16.0$, avoiding the Galactic star contamination. This blue extension cannot be reproduced by any star count models of the Milky Way (see also Bellazzini et al. 2004) and is similar to those observed in the CMD of Local Group (LG) dwarf spheroidal (dSph) galaxies (Draco: Aparicio et al. 2001; Ursa Minor: Carrera et al. 2002). Although it could be produced by blue straggler stars rather than by MS stars of the dwarf galaxy (see discussion in Carrera et al. 2002), the fact that it departs from the MS at $R \sim 19.0$ (fainter than the MS turnoff) is more compatible with the star formation burst hypothesis than the blue stragglers hypothesis, suggesting that the CMa system has had at least two distinct epochs of star formation. The narrow distribution of these blue stars strongly suggests that they are all at a similar distance, which would not be expected if the Galactic warp/flare were the origin of this stellar population. Our diagram also shows evidence of a possible red clump (labeled "RC" in Fig. 1*b*) at $(B - R) \sim 1.5$ and $R \sim 15$, but a suitable control field or radial velocity follow-up is necessary to confirm this overdensity as part of the CMa dwarf. All the CMD features described above can be more easily identified in Figure 1*b*, which shows a synthetic CMD of one of the possible solutions for the stellar population of the CMa dwarf (see § 4.1) overplotted in our observed $[B - R, B]$ CMD.[5] The remarkable similarity of the morphology of this model CMD with the observed one also supports the dwarf nature of CMa.

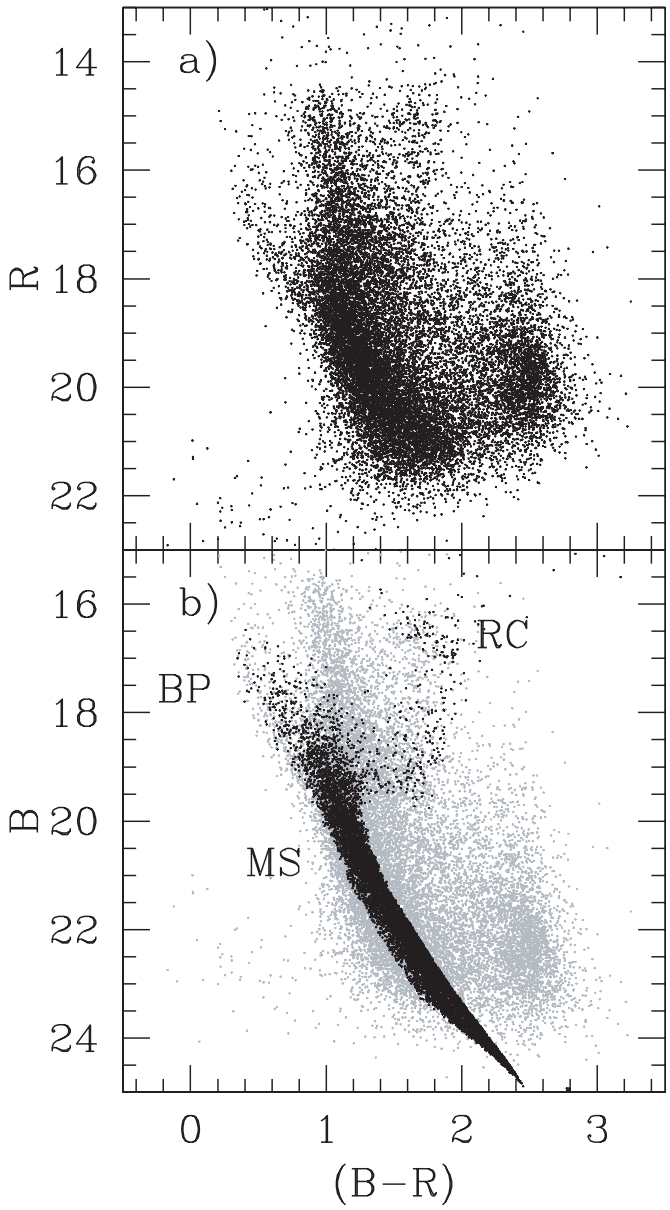

FIG. 1.—(*a*) $(B - R)$ vs. R color-magnitude diagrams of the center of the CMa overdensity based on our short-exposure data (see § 3 for a discussion). (*b*) A synthetic CMD (*black points*) for a metal-rich population (see § 4.1) as a possible solution for the CMa stellar population is overplotted in the observed $(B - R)$ vs. B CMD (gray points). This diagram is only presented here with the illustrative purpose of providing a better identification of those regions of the diagram populated by the brightest stars (red clump [RC], main sequence [MS], and upper MS [BP]) of the putative dwarf galaxy against the Galactic foreground and background contamination. [*See the electronic edition of the Journal for a color version of this figure*.]

Figure 2 shows the $[B - R,\ B]$ CMD based on our long-exposure data. This CMD reveals a prominent, high contrast, and well-populated MS feature extending beyond our limiting magnitude ($B \sim 24.5$). The color width of this MS feature remains

[4] Taken from the WFI Web site; see http://www.ls.eso.org/lasilla/Telescopes/2p2T/E2p2M/WFI/.

[5] This synthetic CMD is used here for a qualitative understanding of the expected features in the CMD of the galaxy population rather than for a quantitative comparison with the data, which is beyond the scope of this paper.

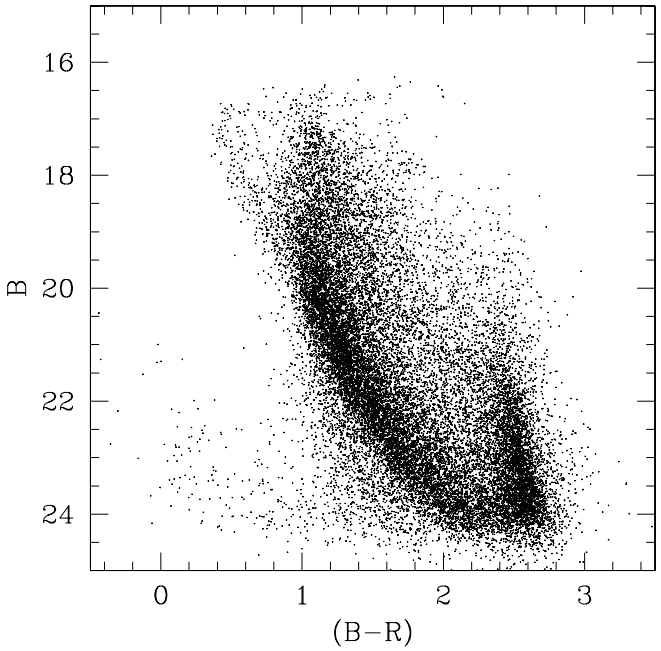

FIG. 2.—$(B - R)$ vs. B color-magnitude diagram of the center of the CMa dwarf galaxy based on our long-exposure data. Photometry of stars brighter than $B \sim 20$ mag suffers larger errors due to CCD saturation, but they were included in the diagram as a guide for matching the MS feature in this figure and in Fig. 1*b*.

roughly constant along a large magnitude range and is comparable to that observed in the CMD of LG dwarf galaxies or massive globular clusters. This evidence strongly confirms the presence of a limited range in distance, and it is therefore associated with a possibly still-bound stellar system; distance, line-of-sight size, and stellar density are investigated in § 4.

4. PROPERTIES OF THE CANIS MAJOR DWARF GALAXY

4.1. *Distance*

Our CMD does not show any unambiguous, convincing signature of the bright, post-MS populations—the red clump (RC), horizontal branch, RR Lyrae stars, or red giant branch stars—that must accompany the clearly detected MS stars. Those post-MS classes of stars have been extensively used to constrain the distance and stellar population properties of LG dwarf galaxies. Consequently, our data are not well suited for a reliable distance estimate to CMa, as there are degeneracies between stellar population assumptions, the reddening and the distance, when considering only the MS in the CMD. In spite of this degeneracy, we try here to set some limits on the distance to the CMa dwarf by fitting the observed MS with synthetic CMDs, assuming some different evolutionary scenarios for the galaxy. However, it is important to stress that these are not the only possible solutions and that more data from alternative distance indicators are necessary to confirm the distance reported in this paper.

Adopting $E(B - V) = 0.213 \pm 0.029$ mag for our field from the Schlegel et al. (1998, hereafter SFD98) dust map, our best model CMD fitting for an old population (age >11 Gyr, with mean $Z = 0.006$) provides an upper limit on the distance modulus of $(m - M)_0 = 13.6 \pm 0.2$ ($d_\odot = 5.3 \pm 0.2$ kpc). For a younger stellar population similar to that reported by Bellazzini et al. (2004; age 4–10 Gyr, with mean $Z = 0.006$), one gets $(m - M)_0 = 14.2 \pm 0.2$ ($d_\odot = 6.9 \pm 0.3$ kpc). However, it has been suggested that the SFD98 dust maps could overestimate the actual reddening of our field (Bonifacio et al. 2000). To check this, we have obtained $E(B - V)$ data for individual stars in the WFI field from a star-by-star interpolation of the SFD98 dust maps. We find that the $E(B - V)$ distribution is skewed, with about 27% of the stars across our CMD affected by $E(B - V) > 0.2$. Therefore, we ignore stars assigned $E(B - V) > 0.3$ because they cannot have a significant effect on our distance and line-of-sight size estimates.[6] For the mean standard deviation of the remaining stars, we obtain $E(B - V) = 0.08 \pm 0.07$ mag. This lower reddening value does not permit an acceptable MS fitting for the two former model CMDs, as both produce MS features that are bluer than observed. An acceptable fitting is obtained by increasing the mean metallicity of the galaxy (mean $Z = 0.01$), yielding a distance modulus of $(m - M)_0 = 14.5 \pm 0.2$ ($d_\odot = 7.9 \pm 0.3$ kpc). This last value is in very good agreement with previous estimates based on different CMD indicators (Bellazzini et al. 2004; Martin et al. 2004b), and it is adopted as the distance to CMa throughout.

4.2. *The Line-of-Sight "Depth" of CMa*

To estimate the line-of-sight extent (or "depth") of CMa, we analyze the observed width of the MS, $\sigma_{\mathrm{MS,total},B}$. Near the MS turnoff the MS is steep, and at the faintest magnitudes measurement errors may dominate the width. Hence, we consider the B-band apparent magnitude distribution of stars in the $(B - R)$ color range of 1.50–1.55 mag, using the long-exposure data (see Fig. 2). We modeled this distribution as the linear sum of two components: (1) the smooth distribution of underlying stars, due to the Galactic warp and thin disk, by a linear function; and (2) the CMa MS, by a Gaussian function, characterized by a standard deviation $\sigma_{\mathrm{MS,total},B}$. Even if all CMa stars were at the same distance, $\sigma^2_{\mathrm{MS,total},B}$ would be nonzero and could be described by the quadrature sum of three components: the intrinsic MS size due to a range of stellar population ages and metallicities,[7] plus contribution to the MS width from observational effects ($\sigma_{\mathrm{MS,int},B}$), and the differential reddening (DR) of the field ($\sigma_{\mathrm{DR},B}$), estimated from the SFD98 dust maps. We then attribute the remaining width of the MS to the distance distribution of the CMa stars ($\sigma_{\mathrm{CMa,depth},B}$). In brief, we fitted the distribution in Figure 3 (in a χ^2 sense) to a linear function at $B = 20$–20.5 and 23.5–24 mag and fitted a Gaussian function in a nonlinear least-squares way after subtracting the linear fit. The fitting was repeated for two adjacent color intervals in order to obtain a statistical uncertainty in the MS width. Their mean and standard deviation data are given in Table 1 together with the rest of the parameters used to determine the line-of-sight size of CMa.

Our best-fitting $\sigma_{\mathrm{MS,total},B}$, converted into kiloparsecs, yields $\sigma_{\mathrm{CMa,depth},B} = 0.8 \pm 0.15$ kpc, or FWHM = 1.95 kpc (see Table 1). Based on 2MASS data, Martin et al. (2004b) report that the angular extent of the overdensity corresponds to a FWHM of ~4.2 kpc (at a heliocentric distance of 7.1 ± 1.3 kpc), significantly larger than the line-of-sight value estimated here. This is not necessarily inconsistent, because severe tidal perturbations may cause a tangential stretching of the CMa dwarf. In addition, the estimated size of the CMa dwarf can provide a reliable estimation of its mass, assuming that bound stellar systems undergoing disruption have a spatial extension similar to or larger than the Jacobi limit, as Peñarrubia et al. (2005) find for the Monoceros

[6] Choosing a smaller cutoff threshold does not have a significant effect on the results presented in this paper.

[7] This was obtained from a synthetic CMD computed for a constant and arbitrary star formation rate between 4 and 10 Gyr and $Z = 0.006$([Fe/H] = −0.48 dex).

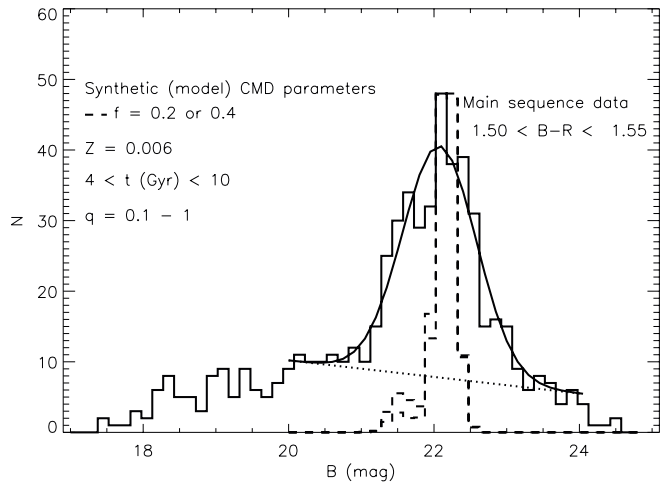

FIG. 3.—*B*-band histogram derived for the $B - R$ range 1.50–1.55 mag in the long-exposure data. The corresponding histogram from a synthetic CMD (4–10 Gyr; $Z = 0.006$) is overlaid (*dashed line*). This synthetic CMD was computed by means of the IAC-STAR interface (Aparicio & Gallart 2004) using the evolutionary library from Girardi et al. (2000) and is considered a binary fraction ("*f*") of 0.2 and 0.4, with a flat probability distribution of mass ratios ("*q*") between 0.1 and 1. The model distributions are indistinguishable. The overplotted bell-shaped curve (*solid line*) is the linear sum of a linear fit to the underlying Milky Way stars (*dotted line*) and a Gaussian fit to the remaining (i.e., CMa MS) histogram. See § 4.2 for further details on data fitting and the MS width.

stream progenitor. In that case (see eq. [7-84] of Binney & Tremaine 1987),

$$M_s \sim 3M(<R_{\rm gal})(R_t/R_{\rm gal})^3,$$

where $M(<R_{\rm gal})$ is the Galaxy mass within $R_{\rm gal}$, and R_t is the Jacobi limit (also called the tidal radius). Adopting $R_t \simeq 1.6$ (which accounts for approximately 96% of the dwarf mass) and the mass profile used by Peñarrubia et al. (2005), we find $M_s > 5 \times 10^8\ M_\odot$, indicating that the present mass of the CMa dwarf should be similar to that predicted by our model of the Monoceros stream progenitor ($3 \times 10^8\ M_\odot$; Peñarrubia et al. 2005).

Finally, in order to compare the size of CMa with those of known dwarf galaxies, we estimate the line-of-sight half-brightness radius, $r_{1/2}$, from the Gaussian model of the line-of-sight profile given in Figure 3. We obtain $r_{1/2} = 0.94 \pm 0.18$ (random) $\pm$ 0.18 (systematic) kpc. This size is in agreement with the model prediction (Peñarrubia et al. 2005), but is significantly bigger than that of several dwarf galaxies in the LG (see Table 4 of Irwin & Hatzidimitriou 1995).

4.3. *Surface Brightness and Absolute Magnitude*

We estimate the central surface brightness (SB) of the CMa dwarf by matching the observed surface density of MS stars to scale those derived from a (candidate) synthetic CMD for the CMa galaxy (2.5–15 Gyr; $Z = 0.006$) for which the integrated magnitude is known. We used the short-exposure data and counted stars on the upper MS in a small box such that $1 < B - R < 1.5$ and $18 < R < 19$; the position of this CMD box allows for a significant sample of the dominant CMa stellar population. To correct the MS star counts for contamination of Milky Way stars, we use the CMD of a control field obtained at the Galactic position $(l,\ b) = (240, +15)$, taken from our recent survey to investigate the extent and stellar population of the CMa dwarf (D. J. Butler et al. 2005, in preparation). We used star counts from the red plume region of thick disk MS stars (where $0.5 < B - R < 1.5$ and $15 < R < 16.5$) in the control and CMa fields to subtract a scaled contamination level from the CMa MS star selection box mentioned above. We find $\mu_{V,0} = 23.3 \pm 0.1$ mag arcsec^{-2} (taken as the intensity-weighted average of $\mu_{B,0}$ and $\mu_{R,0}$), where the SB uncertainty was estimated by taking Poisson statistical errors in the star counts. That value is very similar to those of Milky Way dSph satellites (Mateo 1998) and provides further evidence that we have detected a part of the main body of a dwarf galaxy and not a piece of a possible tidal stream, whose typical SB would be expected to lie in the range of 30.0 to 31.5 mag arcsec^{-2} (Johnston et al. 1999).

To estimate the total *V*-band luminosity, we use an exponential SB profile with a (near-IR) scale length of 0.73 ± 0.05 kpc (Martin et al. 2004a), with the mean heliocentric distance taken to be 7.1 kpc. We obtained $M_V = -14.5 \pm 0.1$ mag, corresponding to a total *V*-band intensity $\log(I_V/I_{V,\odot}) = 7.7 \pm 0.1$. This yields a total mass for the satellite of $M/M_\odot = 5 \times 10^7 \Gamma$ [where $\Gamma = (M/M_\odot)/(L/L_\odot)$]. Assuming the mass-to-light ratio of CMa is in the range $4 < \Gamma < 22$ in solar units (which contains the majority of the LG dSphs), the present remnant of the CMa dwarf would have a total mass of $2.0 \times 10^8 < M/M_\odot < 1.1 \times 10^9$, consistent with the value obtained from the observational extension of the satellite and from the prediction of our theoretical simulations (see § 4.2). The combination of this luminosity with the size derived in § 4 places this stellar system among the dwarf galaxies in the L_V-size plane (see Fig. 5 of Pasquali et al. 2005). In addition, CMa follows the well-defined $M_V - \mu_V$ relationship shown by Caldwell (1999) for dwarf galaxies. However, assuming the stellar component of the galaxy has an average metallicity of [Fe/H] ~ -0.4 (Bellazzini et al. 2004), this galaxy is, like the Sagittarius dSph, an outlier of the well-known [Fe/H] $- M_V$

TABLE 1

BUDGET USED TO DETERMINE THE THICKNESS OF THE CMa MS, AND AN MS MODEL WITH $Z = 0.006$ AND AGE OF 4 TO 10 Gyr

Parameter	Value
Total observed main-sequence width, $\sigma_{\rm MS,\,total,\,B}$ (mag)	0.57 ± 0.06
Random Errors:	
$\sigma_{\rm MS,\,int,\,B}$ (mag)	0.19[a]
$\sigma_{\rm DR,\,B}$ (mag)	0.29[b]
Systematic Error:	
Model MSTO (adopted error)	0.1
Photometry calibration	0.07

[a] Observational effect estimated from artificial star tests, based on a single age population, and determined at $B \sim 22.1$ mag and $B - R = 1.5$ to 1.55 mag.
[b] Adopted the Cardelli et al. (1989) reddening law and $E(B - V) = 0.08$ mag (see § 4.1).

TABLE 2

RELEVANT PROPERTIES OF THE CMa FIELD

Parameter	Value
l (deg)	240.15
b (deg)	−08.07
$E(B - V)$ (mag)	0.08 ± 0.07
d (kpc)	7.9 ± 0.3[a]
Δd (kpc)	1.60 ± 0.30[b]
$r_{1/2}$ (kpc)	0.9 ± 0.3
$\mu_{V,0}$ (mag arcsec^{-2})	23.3 ± 0.1[c]

[a] Model used: $Z = 0.001$, 4–10 Gyr, $f = 0.2$, and $q = 0.1$–1.
[b] 2 σ line-of-sight size.
[c] Model used: $Z = 0.006$, 4–10 Gyr, $f = 0.2$, and $q = 0.1$–1.

relation, since it is too metal-rich for its estimated absolute magnitude. This suggests, as in the case of Sagittarius, that a different mechanism (possibly tidal stripping) is predominantly driving its star formation history.

Derived parameters for the CMa overdensity are given in Table 2.

5. CONCLUSIONS

From our data we have established that the putative center of CMa is a very high contrast density feature that has a very narrow radial extent, $r_{1/2}/R_{GC} < 0.1$. These results strongly support the interpretation of a distinct, possibly still bound, stellar system whose properties are consistent with those expected for the remnant of a partially disrupted dwarf satellite. In turn, the high density contrast and the limited line-of-sight extent of the CMa are very difficult to reconcile (if at all) with a flared or warped Galactic disk viewed in projection (Momany et al. 2004). Although the obtained properties for the satellite (Table 2) in this study are subject to considerable uncertainties (e.g., stellar population, Galactic contamination, and radial profile), they are in agreement with those of the known Milky Way dSph satellites (Mateo 1998) and with the known size-luminosity relation followed by Milky Way dwarf spheroidals.

At a distance of 8 kpc, CMa is the closest dwarf galaxy known. It may be not only the parent of the Galactic low-latitude stellar stream, but also a unique laboratory for testing galaxy evolution theories. In particular, our CMD shows the availability for the first time of thousands of MS stars of different ages in a magnitude range suited to high-resolution spectroscopy-based abundance studies using 4 m class telescopes. This will allow one to study the star formation history of a dwarf galaxy with unprecedented spectral resolution and is therefore a top candidate for chemodynamical modeling of dwarf galaxy evolution in the Galaxy.

We thank A. Robin, E. D. Skillman, and the referee H. Rocha-Pinto for their useful comments. D. M.-D. dedicates this work to the memory of his grandfather, Manuel Delgado-Membrives.

REFERENCES

Aparicio, A., Carrera, R., & Martínez-Delgado, D. 2001, AJ, 122, 2524
Aparicio, A., & Gallart, C. 2004, AJ, 128, 1465
Bellazzini, M., Ibata, R., Monaco, L., Martin, N., Irwin, M. J., & Lewis, G. F. 2004, MNRAS, 354, 1263
Binney, J., & Tremaine, S. 1987, Galactic Dynamics (Princeton: Princeton Univ. Press)
Bonifacio, P., Monai, S., & Beers, T. C. 2000, AJ, 120, 2065
Caldwell, N. 1999, AJ, 118, 1230
Cardelli, J. A., Clayton, G. C., & Mathis, J. S. 1989, ApJ, 345, 245
Carrera, R., Aparicio, A., Martínez-Delgado, D., & Alonso-García, J. 2002, AJ, 123, 3199
Girardi, L., Bressan, A., Bertelli, G., & Chiosi, C. 2000, A&AS, 141, 371
Irwin, M., & Hatzidimitriou, D. 1995, MNRAS, 277, 1354
Johnston, K. V., Zhao, H., Spergel, D. N., & Hernquist, L. 1999, ApJ, 512, L109
Majewski, S. R. 2004, in ASP Conf. Ser. 327, Satellites and Tidal Streams, ed. F. Prada, D. Martínez-Delgado, & T. J. Mahoney (San Francisco: ASP), 63
Martin, N. F., Ibata, R. A., Bellazzini, M., Irwin, M. J., Lewis, G. F., & Dehnen, W. 2004a, MNRAS, 348, 12
Martin, N. F., Ibata, R. A., Conn, B. C., Lewis, G. F., Bellazzini, M., Irwin, M. J., & McConnachie, W. 2004b, MNRAS, 355, L33
Mateo, M. L. 1998, ARA&A, 36, 435
Momany, Y., Zaggia, S. R., Bonifacio, P., Piotto, G., De Anfeli, F., Bedin, L. R., & Carraro, G. 2004, A&A, 421, L29
Navarro, J. F. 2004, preprint (astro-ph/0405497)
Newberg, H. J., et al. 2003, ApJ, 596, L191
Pasquali, A., Larsen, S., Ferreras, I., Gnedin, O. Y., Malhotra, S., Rhoads, J. E., Pirzkal, N., & Walsh, J. R. 2005, AJ, 129, 148
Peñarrubia, J., et al. 2005, ApJ, 626, 128
Schlegel, D. J., Finkbeiner, D. P., & Davis, M. 1998, ApJ, 500, 525 (SFD98)
Stetson, P. B. 1994, PASP, 106, 205
Yanny, B., et al. 2003, ApJ, 588, 824